Am J Physiol Cell Physiol 287: C1667–C1678, 2004.
First published August 25, 2004; doi:10.1152/ajpcell.00265.2004.

Erythropoietin-modulated calcium influx through TRPC2 is mediated by phospholipase Cγ and IP_3R

Qin Tong,[1,3] Xin Chu,[3] Joseph Y. Cheung,[2,3] Kathleen Conrad,[1,3] Richard Stahl,[3] Dwayne L. Barber,[4] Gregory Mignery,[5] and Barbara A. Miller[1,3]

[1]*Departments of Pediatrics and* [2]*Cellular and Molecular Physiology, The Pennsylvania State University College of Medicine, Hershey, Pennsylvania 17033;* [3]*The Henry Hood Research Program, The Sigfried and Janet Weis Center for Research, The Geisinger Clinic, Danville, Pennsylvania 17822;* [4]*Division of Cellular and Molecular Biology, Ontario Cancer Institute, Toronto, Ontario M5G 2M9, Canada; and* [5]*Department of Physiology, Stritch School of Medicine, Loyola University Chicago, Maywood, Illinois 60153*

Submitted 2 June 2004; accepted in final form 18 August 2004

Tong, Qin, Xin Chu, Joseph Y. Cheung, Kathleen Conrad, Richard Stahl, Dwayne L. Barber, Gregory Mignery, and Barbara A. Miller. Erythropoietin-modulated calcium influx through TRPC2 is mediated by phospholipase Cγ and IP_3R. *Am J Physiol Cell Physiol* 287: C1667–C1678, 2004. First published August 25, 2004; doi:10.1152/ajpcell.00265.2004.—In the present study, we examined the mechanisms through which erythropoietin (Epo) activates the calcium-permeable transient receptor potential protein channel (TRPC)2. Erythroblasts were isolated from the spleens of phenylhydrazine-treated mice, and Epo stimulation resulted in a significant and dose-dependent increase in intracellular calcium concentration ($[Ca^{2+}]_i$). This increase in $[Ca^{2+}]_i$ was inhibited by pretreatment with the phospholipase C (PLC) inhibitor U-73122 but not by the inactive analog U-73343, demonstrating the requirement for PLC activity in Epo-modulated Ca^{2+} influx in primary erythroid cells. To determine whether PLC is involved in the activation of TRPC2 by Epo, cell models were used to examine this interaction. Single CHO-S cells that expressed transfected Epo receptor (Epo-R) and TRPC2 were identified, and $[Ca^{2+}]_i$ was quantitated. Epo-induced Ca^{2+} influx through TRPC2 was inhibited by pretreatment with U-73122 or by downregulation of PLCγ1 by RNA interference. PLC activation results in the production of inositol 1,4,5-trisphosphate (IP_3), and TRPC2 has IP_3 receptor (IP_3R) binding sites. To determine whether IP_3R is involved in Epo-R signaling, TRPC2 mutants were prepared with partial or complete deletions of the COOH-terminal IP_3R binding domains. In cells expressing TRPC2 IP_3R binding mutants and Epo-R, no significant increase in $[Ca^{2+}]_i$ was observed after Epo stimulation. TRPC2 coassociated with Epo-R, PLCγ, and IP_3R, and the association between TRPC2 and IP_3R was disrupted in these mutants. Our data demonstrate that Epo-R modulates TRPC2 activation through PLCγ; that interaction of IP_3R with TRPC2 is required; and that Epo-R, TRPC2, PLCγ, and IP_3R interact to form a signaling complex.

transient receptor potential protein channels; erythropoietin receptor; calcium channels

ERYTHROPOIETIN IS A GLYCOPROTEIN that is obligatory for the proliferation and differentiation of erythroid cells, and the erythropoietin (Epo) receptor (Epo-R) is a member of the large superfamily cytokine receptors, which share many signal transduction pathways. Epo stimulates a dose-dependent increase in the intracellular free calcium ($[Ca^{2+}]_i$) that is mediated through a voltage-independent ion channel (9, 10, 14), and recently Epo has been shown to modulate Ca^{2+} influx through the transient receptor potential (TRP) protein family member TRPC2 (11, 12). Ca^{2+} is a universal intracellular second messenger that influences many cell functions (3). Determination of the signaling pathways through which Epo-R modulates Ca^{2+} influx through TRPC2 is important in understanding erythroid proliferation and differentiation and is likely to be widely applicable to other cytokine receptor pathways.

The TRP protein superfamily comprises a diverse group of voltage-independent Ca^{2+}-permeable cation channels that are related to the archetypal *Drosophila* TRP and expressed in mammalian cells (15, 35–37). Many mammalian TRP channels (TRPC) are activated after stimulation of receptors, and most of these receptors activate different isoforms of phospholipase C (PLC) (15, 36, 37). Activation of PLC results in hydrolysis of phosphatidylinositol 4,5-bisphosphate (PIP_2) to inositol 1,4,5-trisphosphate (IP_3) and diacylglycerol (DAG). Some TRPC are Ca^{2+} store release operated: one proposed mechanism of activation is that IP_3-mediated release of Ca^{2+} from internal stores results in a conformational change in IP_3 receptors (IP_3R), inducing a conformational change and opening of the store-operated TRPC (36). However, a direct interaction between TRPC and IP_3R was recently demonstrated for all TRPC and for all IP_3R (6, 19, 20, 29, 42). High IP_3 concentrations in the vicinity of IP_3R, resulting from close association of IP_3R with PLC-coupled receptors, have been proposed to directly activate IP_3R and the associated TRPC (13). For TRPC2, interaction with IP_3R type III in the vomeronasal (VMO) organ has been reported (7). Some TRPC (TRPC3, TRPC6) can also be activated by DAG (16, 28, 30, 45).

Epo binding activates Epo-R by inducing a conformational change in Epo-R, resulting in activation of Jak2 through transphosphorylation (21). Jak2 subsequently phosphorylates some or all of the eight tyrosines in the intracellular domain of Epo-R, and phosphorylation of tyrosine residues on Epo-R attracts other intracellular proteins to bind to Epo-R via SH2 domains (21, 47). Epo stimulation of its receptor induces tyrosine phosphorylation and activation of both PLCγ1 and PLCγ2 (5, 31, 32, 40). In addition, Epo stimulation results in the production of IP_3 (40) and DAG (2).

In the present study, we examined the mechanism of activation of TRPC2 by Epo. In both primary erythroblasts and Chinese hamster ovary (CHO)-S cells transfected with Epo-R

Address for reprint requests and other correspondence: B. A. Miller, Dept. of Pediatrics, Milton S. Hershey Medical Center, PO Box 850, Hershey, PA 17033 (E-mail: bmiller3@psu.edu).

The costs of publication of this article were defrayed in part by the payment of page charges. The article must therefore be hereby marked "*advertisement*" in accordance with 18 U.S.C. Section 1734 solely to indicate this fact.

and TRPC2, Epo stimulated a significant increase in $[Ca^{2+}]_i$. Epo-induced $[Ca^{2+}]_i$ increase was inhibited by pretreatment with the PLC inhibitor U-73122 and by downregulation of PLCγ1 with RNA interference (RNAi), demonstrating the requirement for PLC activity in Epo-modulated Ca^{2+} influx. In cells transfected with Epo-R and TRPC2 mutants with deletions of IP_3R binding sites, Epo failed to stimulate a significant rise in $[Ca^{2+}]_i$, demonstrating the requirement for IP_3R interaction with TRPC2 in Epo-induced Ca^{2+} influx. TRPC2 constitutively associated with Epo-R, PLCγ1, and IP_3R. These data suggest the existence of a signaling complex consisting of Epo-R, PLCγ, IP_3R, and TRPC2. They support the conclusion that after Epo stimulation, PLCγ activation produces IP_3, which activates IP_3R, and IP_3R interaction with TRPC2 contributes to and is required for channel opening.

EXPERIMENTAL PROCEDURES

All experimental procedures were performed in accordance with the "Guiding Principles in the Care and Use of Animals" of the American Physiological Society.

Tissue and cells lines. CHO-S cells were cultured in Dulbecco's modified Eagle's medium (DMEM) with 10% fetal calf serum (FCS) and 0.1 mM nonessential amino acids. Human embryonic kidney (HEK)-293T cells were cultured in DMEM with 10% FCS. Splenic erythroblasts were obtained by injecting C57Bl/6 mice (8–12 wk of age) with phenylhydrazine (60 mg/kg) intraperitoneally on *days 1* and *2* (1, 22). Mice were killed on *day 5* by cervical dislocation, the spleens removed, and single-cell suspensions were prepared. To separate splenic erythroid cells into different stages of maturation, the spleen cell suspensions were washed and labeled with TER-119 MicroBeads (10 μl/1 × 10^7 cells; Miltenyi Biotech, Auburn, CA). TER-119$^-$ (erythroid progenitors and early precursors) and TER-119$^+$ cells (more mature nucleated erythroblasts and erythrocytes) were selected by magnetic sorting with the VarioMACS (Miltenyi Biotech) as described previously (12, 18). Wright's staining and immunofluorescence confirmed that >90% of TER-119$^-$ and TER-119$^+$ nucleated cells were erythroid (12).

Transfection of mTRPC and Epo-R into CHO-S cells. TRPC2 clone 14 (c14) (44), TRPC2 with IP_3R binding mutants, and rat TRPV1 (8) were subcloned into pcDNA3, pQBI50 (QbioGene, Carlsbad, CA), or pcDNA3.1/V5-His TOPO (Invitrogen, Carlsbad, CA). Other constructs were used in some experiments (see below). CHO-S cells at 50–70% confluence were transfected with these vectors and/or pTracer-CMV expressing Epo-R with the use of Lipofectamine Plus (Invitrogen) or Lipofectamine 2000 in accordance with the manufacturer's recommended transfection protocols (11). CHO-S cells were routinely studied 48 h after transfection.

Measurement of $[Ca^{2+}]_i$ with digital video imaging. The fluorescence microscopy-coupled digital video imaging system used to measure changes in $[Ca^{2+}]_i$ was described previously (9–11, 33, 34). After isolation and separation with the VarioMACS, TER-119$^-$ splenic erythroblasts were incubated in Iscove's modified Dulbecco's medium (GIBCO-BRL, Grand Island, NY) containing 2% FCS and 50 μM β-mercaptoethanol for 2–4 h without growth factor. Splenic erythroblasts were then adhered to fibronectin-coated glass coverslips and loaded for 20 min with 0.1 μM fura-2 AM (Molecular Probes, Eugene, OR). For some experiments, the active PLC inhibitor U-73122 (0.1–2.5 μM; Sigma, St. Louis, MO) or the inactive inhibitor U-73343 (Sigma) were included in the buffer during fura-2 loading and during Epo stimulation. Fura-2-loaded cells were visualized with digital video imaging, and fluorescence was quantitated by using the fluorescence intensity ratio (R) of the emission (510 nm) measured after excitation at 350 nm divided by the emission after excitation at 380 nm. The free intracellular calcium concentration ($[Ca^{2+}]_i$) was calculated from fura-2 fluorescence signals using the in vivo calibration method and the equation

$$[Ca^{2+}]_i = K'_d[(R - R_{min})/(R_{max} - R)] \cdot (S_{f2}/S_{b2}),$$

where K'_d is the Ca^{2+} fura-2 dissociation constant (224 nmol/l) and S_{f2}/S_{b2} was obtained as described previously (33). $[Ca^{2+}]_i$ of individual cells was measured at baseline and at intervals over 25 min after stimulation with 0–40 U/ml of recombinant Epo (2,000 U/ml; Amgen, Thousand Oaks, CA).

We were not able to use fura-2 as the detection fluorophore to study changes in $[Ca^{2+}]_i$ in transfected cells, because its excitation and emission wavelengths overlap with those of green fluorescent protein (GFP). Instead, we used the fluorescent indicator fura red (excitation, 440 and 490 nm; emission, 600 nm long pass), a dual-wavelength excitation probe (12, 23, 48). Transfected CHO-S cells grown on glass coverslips were loaded at 48 h with 5 μM fura red for 20–25 min at 37°C in the presence of Pluronic F-127. Cells were treated with 0 or 40 U/ml of Epo. In some experiments, 680 μM MnCl was substituted in the extracellular buffer for CaCl. In others, cells were exposed to 3.5 μM thapsigargin after baseline $[Ca^{2+}]_i$ measurements or to 0.1–10 μM U-73122 or U-73343 during fura red loading and during Epo stimulation. $[Ca^{2+}]_i$ was measured by determining of the fluorescence intensity ratio R (F_{440}/F_{490}), which was measured at intervals of 5 s for the first 30 s, intervals of 5–15 s for the next 2–4 min, and at 2- to 5-min intervals over the remaining 20-min time course after treatment with PBS or Epo. We calibrated the constants S_{f2}, S_{b2}, and K'_d of fura red and measured R_{min} and R_{max} for fura red as described previously (12). $[Ca^{2+}]_i$ was calculated using the same formula used for calculations with fura-2.

Statistical significance of results was analyzed by performing one-way analysis of variance. In experiments with HEK-293T cells, the cells were transfected under conditions identical to those used for CHO-S cells. HEK-293T cells were loaded 48 h after transfection with 2.5 μM fura red and $[Ca^{2+}]_i$ measured as described for CHO-S cells.

Downregulation of PLCγ with RNAi. To reduce endogenous expression of PLCγ, PLCγ1 *SMART*pool small interfering RNA (siRNA) reagent (no. 60–034; Upstate, Charlottesville, VA) targeted to human PLCγ1 was cotransfected into HEK-293T cells with Epo-R in pTracer-CMV and TRPC2 c14 in pQBI50 (24). NonSpecific Control *SMART*pool siRNA reagent was cotransfected in control cells. SiRNA reagents were transfected using the manufacturer's recommended protocol at a final concentration of 200 pmol/35-mm dish, with Lipofectamine Plus used as the transfection reagent. At 48 h, cells were used for $[Ca^{2+}]_i$ measurements or for Western blotting.

Immunolocalization of TRPC2, Epo-R, PLCγ, and IP_3R in primary erythroid cells and transfected CHO-S cells. TER-119$^-$ splenic erythroblasts (3 × 10^5 cells/chamber) were placed in each well of Lab-Tek Permanox chamber slides precoated with fibronectin. After 45 min, cells were washed twice with PBS, fixed in methanol at −20°C for 10 min, and permeabilized in 0.5% Triton X-100 in PBS for 2 min. Blocking was performed by incubating cells for 10 min in 5% milk. Cells were then stained with the primary antibodies anti-TRPC2 c14 (11), anti-Epo-R (sc-697, Santa Cruz Biotechnology, Santa Cruz, CA), anti-PLCγ1 (1249; Santa Cruz Biotechnology), anti-IP_3R type II (sc-7278; Santa Cruz Biotechnology), and/or anti-IP_3R type III (sc-7277; Santa Cruz Biotechnology) at 1:50 for 45 min at room temperature, followed by the appropriate secondary antibody (donkey anti-rabbit Alexa 488, donkey anti-goat Alexa 594; Molecular Probes) for 2 h in the dark. Cells were stained with 4,6-diamidino-2-phenylindole in Vectashield mounting medium (Vector Laboratories, Burlingame, CA) for visualization. Images were acquired with the Leica TCS SP2 confocal microscope.

For immunolocalization experiments with TRPC2 IP_3R binding mutants, CHO-S cells were cotransfected with TRPC2 or TRPC2 IP_3R binding mutants in pQBI50 or in pcDNA3.1/V5-His TOPO, IP_3R type II in pcDNA3, Epo-R in pTracer-CMV, or combinations of

these plasmids. For these experiments, a blue fluorescent protein (BFP) tag was substituted for the GFP tag in pTracer-CMV so that GFP would not interfere with Alexa 488 fluorescence. Cells were stained as described above for primary erythroblasts. Either goat or donkey anti-rabbit Alexa 488, donkey anti-goat Alexa 594, or goat anti-mouse Alexa 594 antibodies (1:200 and 1:50 dilutions, respectively; Molecular Probes) were used as the secondary antibodies where appropriate.

Immunoblotting of whole cell lysates and crude membrane preparations. Cell pellets from TER-119$^-$ and TER-119$^+$ splenic erythroblasts, CHO-S cells, or HEK-293T cells were removed from storage at −80°C. For Western blotting of whole cell lysates, cell pellets were suspended in lysis buffer, and Western blotting was performed as previously described (12). After blocking, nitrocellulose membranes were incubated with anti-TRPC2 c14 (1:400), anti-Epo-R (1:200), anti-PLCγ1 (1:200), or anti-IP$_3$R type II (1:100 dilution) antibodies. Blots were then washed and incubated with horseradish peroxidase (HRP)-conjugated anti-rabbit or anti-goat antibodies (1:2,000 dilution). Enhanced chemiluminescence (ECL) was used for signal detection.

For crude membrane preparations, cell pellets were suspended in *buffer I* (10 mM Tris·HCl, pH 7.4, and 1× protease inhibitor cocktail) and sonicated. An equal volume of *buffer II* (10 mM Tris·HCl, pH 7.4, 300 mM KCl, 20% sucrose, and 1× protease inhibitor mixture) was added. The suspension was then centrifuged at 10,000 *g* for 10 min at 4°C, and the supernatant was spun at 100,000 *g* for 1 h at 4°C. Crude membranes were solubilized in buffer containing 62 mM Tris·HCl (pH 6.8), 2% SDS, and 10% glycerol. Protein was quantified and Western blotting was performed as described above.

Immunoprecipitation. To determine whether mTRPC2 associates with Epo-R, PLCγ, or IP$_3$R, CHO-S cells were transfected with mTRPC2 c14 (in pcDNA3.1/V5His TOPO), mEpo-R (in pcDNA3), rat PLCγ1 (in pcDNA3), rat IP$_3$R type II (in pcDNA3) (39), or combinations of these vectors. Lysates were prepared from cell pellets with lysis buffer containing 50 mM Tris, pH 7.5, 150 mM NaCl, 1% Triton-X, 1 mM EDTA, and 1× protease inhibitor cocktail. Protein lysates were incubated with preimmune rabbit serum, anti-V5 (Invitrogen), anti-Epo-R, anti-PLCγ1, or anti-IP$_3$R type II antibodies for 2 h at room temperature. Protein A/G PLUS Agarose beads (Santa Cruz Biotechnology) were then added for 1 h at room temperature with mixing, and immunoprecipitates were washed three times. Sample buffer (2×) was added to the pellets, and the samples were boiled. Western blotting was performed as described above, and blots were probed with anti-V5 (1:2,000 dilution; Invitrogen), anti-Epo-R, anti-PLCγ1, anti-IP$_3$R type II, or anti-actin (Sigma) antibodies, followed by the appropriate HRP-conjugated secondary antibodies and ECL.

As a control for the specificity of immunoprecipitation, a mutant rat TRPV1 gene (8) (gift from Dr. Jan Teisinger, Institute of Physiology, Academy of Sciences, Prague, Czech Republic) was prepared in which the NH_2 terminus including the single putative PLCγ SH3 binding domain at amino acid (aa) 38 was deleted. A nucleotide sequence encoding methionine was substituted for that of proline at aa 38, and the normal TRPV1 protein coding sequence began with aa 39. This sequence was subcloned into the pcDNA3.1/V5His TOPO vector. Cells were cotransfected with mutant TRPV1, mEpo-R, and rat PLC in control immunoprecipitation studies.

For immunoprecipitation with TER-119$^-$ erythroblasts, protein lysates were incubated with preimmune serum, anti-PLCγ1 (4 ug), or anti-Epo-R (4 μg) antibodies for 3 h at 4°C with mixing. Protein A/G PLUS-Agarose beads were then added for 30 min, followed by centrifugation of beads and washing. Sample buffer was added to the pellets, followed by boiling and loading of the supernatant onto gels for protein electrophoresis.

RESULTS

Erythropoietin modulation of Ca^{2+} influx in primary erythroblasts is dependent on PLCγ. Epo previously was shown to activate PLCγ1 and PLCγ2 (5, 26, 31, 40). Because many TRPC are activated through PLC (15, 36), the role of PLCγ in Epo-modulated Ca^{2+} influx in primary erythroblasts was examined. Splenic erythroblasts were isolated from the spleens of phenylhydrazine-treated mice. Epo has been demonstrated to stimulate an increase in $[Ca^{2+}]_i$ in these cells, and the percentage of cells that respond is greater in TER-119$^-$ erythroblasts (less mature erythroid precursors) than in TER-119$^+$ cells (more mature erythroid precursors) (12). To examine the role of PLC in Epo modulation of Ca^{2+} influx in primary erythroid cells, TER-119$^-$ erythroblasts were loaded with fura-2 and stimulated with Epo. Epo stimulated a modest but significant increase in $[Ca^{2+}]_i$ in these cells (55 ± 4% above baseline, 19 cells studied; $P < 0.0001$) compared with cells treated with vehicle (PBS) alone (11 ± 6%, 10 cells studied), similar to results published previously (12). Pretreatment with 2.5 μM of the active PLC inhibitor U-73122 for 20 min abolished the increase in $[Ca^{2+}]_i$ observed after Epo stimulation (8 ± 2% increase above baseline, 10 cells studied). The increase in $[Ca^{2+}]_i$ in cells pretreated with the inactive PLC inhibitor U-73343 was equivalent to that observed after Epo stimulation of untreated cells. These data suggest that PLC is required for Epo-stimulated Ca^{2+} influx in primary erythroblasts.

Subcellular localization of TRPC2, PLCγ, and IP$_3$R in primary erythroblasts. We previously demonstrated that Epo stimulation regulates Ca^{2+} influx through TRPC2 (11, 12). To examine the subcellular localization of TRPC2, Epo-R, PLCγ, and IP$_3$R in primary murine erythroid cells, TER-119$^-$ erythroblasts were costained with anti-TRPC2 c14 or anti-Epo-R or anti-PLCγ1 (rabbit) antibodies as well as anti-IP$_3$R type II (goat), followed by appropriate secondary antibodies. Representative results of immunofluorescence observed with confocal microscopy are shown in Fig. 1. Endogenous TRPC2 (Fig. 1*A*), IP$_3$R type II (Fig. 1, *B*, *E*, and *H*), and PLCγ1 (Fig. 1*G*) were found at or near the plasma membrane but also throughout the cell. Epo-R (Fig. 1*D*) localized at or near the plasma membrane in primary erythroid cells. TER-119$^-$ cells were also stained with anti-IP$_3$R type III antibody; IP$_3$R type III was not detected and was not studied further. Colocalization studies were limited because the majority of available antibodies to these proteins are produced in rabbits (anti-TRPC2, anti-Epo-R, and anti-PLCγ1) or are murine and thus could not be used in the present study. However, the merger of confocal images obtained when costaining with anti-TRPC2, anti-Epo-R, or anti-PLCγ1, and anti-IP$_3$R type II antibodies, demonstrated that TRPC2 (Fig. 1*C*), Epo-R (Fig. 1*F*), and PLCγ1 (Fig. 1*I*) all partially colocalized with IP$_3$R type II. These data demonstrate that TRPC2, Epo-R, PLCγ1, and IP$_3$R have similar localization in primary erythroid cells.

To confirm these studies, crude membranes were prepared from lysates of TER-119$^-$ and TER-119$^+$ erythroblasts, nontransfected CHO-S cells, and CHO-S cells transfected with IP$_3$R type II, PLCγ1, TRPC2 c14, and Epo-R in pcDNA3. Western blotting was performed on protein isolated in the membrane pellets. IP$_3$R type II, PLCγ1, TRPC2, and Epo-R all localized at least partially in the membrane fraction of TER-119$^-$ erythroblasts. This was also observed in transfected

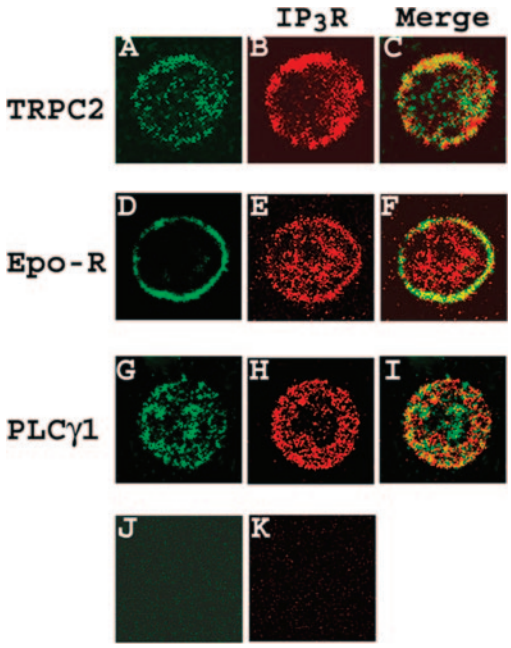

Fig. 1. Immunolocalization of transient receptor potential protein channel (TRPC)2, erythropoietin (Epo) receptor (Epo-R), phospholipase C (PLC)γ1, and inositol 1,4,5-trisphosphate (IP_3) receptor (IP_3R) type II in TER-119$^-$ erythroblasts. TER-119$^-$ erythroblasts adherent to glass slides were stained with anti-TRPC2 clone 14 (c14) (*A*), anti-Epo-R (*D*), anti-PLCγ1 (*G*), and/or anti-IP_3R type II (*B*, *E*, and *H*) antibodies, or nonimmune rabbit serum (*J* and *K*). Donkey anti-rabbit Alexa 488 (anti-TRPC2, anti-Epo-R, anti-PLCγ1) or donkey anti-goat Alexa 594 (anti-IP_3R type II) was used as the secondary antibody. Merged images of Alexa 488 and Alexa 594 are shown in *C*, *F*, and *I*. Sections in midplane were obtained using confocal microscopy. *J*: cells stained with secondary donkey anti-rabbit Alexa 488 antibody. *K*: cells stained with secondary donkey anti-goat Alexa 594 antibody.

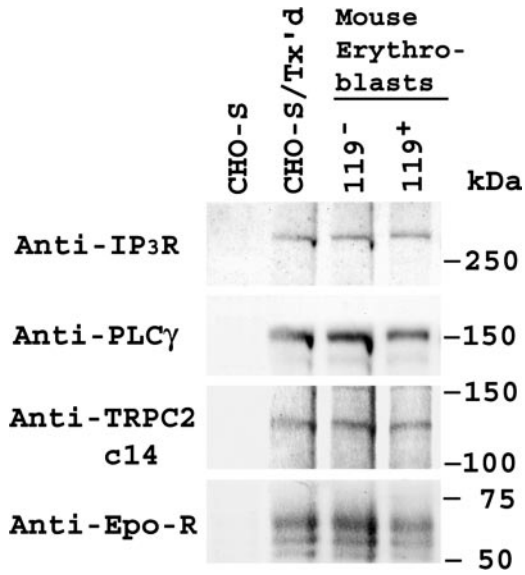

Fig. 2. Western blotting of IP_3R type II, PLCγ1, TRPC2, and Epo-R in murine erythroblasts. Western blotting was performed on membranes prepared from TER-119$^-$ and TER-119$^+$ erythroblasts, nontransfected Chinese hamster ovary (CHO)-S cells, and CHO-S cells transfected with IP_3R type II, PLCγ1, TRPC2 c14, and Epo-R. Blots were probed with anti-IP_3R type II, anti-PLCγ1, anti-TRPC2 c14, or anti-Epo-R antibodies, followed by enhanced chemiluminescence (ECL).

CHO-S cells, which were used as positive controls (Fig. 2). For CHO-S cells in which protein was overexpressed, the amount of protein loaded was ~30% of that loaded for murine erythroblasts. After longer exposure, endogenous PLCγ1 was detected in the membranes of CHO-S cells.

Epo-induced $[Ca^{2+}]_i$ rise is mediated by extracellular Ca^{2+} influx. We previously established a system to examine regulation of Ca^{2+} influx through individual TRPC (11, 12). Single CHO-S cells were transfected with wild-type Epo-R in pTracer-CMV and with TRPC2 in pQBI50. The pTracer-CMV vector contains an SV40 promoter that drives expression of the GFP gene and a cytomegalovirus (CMV) promoter that drives expression of mEpo-R. The pQBI50 vector contains a CMV promoter that drives the expression of SuperGlo BFP infused through a flexible linker to TRPC2. For digital video imaging, successful transfection of individual CHO-S cells with Epo-R was verified by detection of GFP (excitation, 478 nm; emission, 535 nm). Successful transfection of TRPC2 was confirmed by detection of BFP (excitation, 380 nm; emission, 435 nm). Cotransfection of Epo-R and TRPC2 into CHO-S cells permits the study of interaction of Epo-R specifically with TRPC2 and of the regulation of TRPC2. We previously demonstrated that Epo stimulation of CHO-S cells transfected with TRPC2 and Epo-R resulted in a significant increase in $[Ca^{2+}]_i$ (Table 1; $P < 0.0002$) (11, 12). We performed experiments to characterize the rise in $[Ca^{2+}]_i$ stimulated by Epo through TRPC2. Ca^{2+} influx was examined by stimulating cells with Epo in the presence of extracellular Mn^{2+} rather than Ca^{2+}. Influx of Mn^{2+} was monitored by the decrease in fluorescence near the fura red Ca^{2+}-insensitive isosbestic point (458 nm) (16, 48). Representative examples of the time course of Mn^{2+} quenching of fura red fluorescence are shown in Fig. 3. Epo stimulation of CHO-S cells transfected with Epo-R (Fig. 3*B*) or TRPC2 c14 (Fig. 3*C*) resulted in no significant change in fura

Table 1. *PLC is required for Epo-stimulated calcium influx through TRPC2 in transfected CHO-S cells*

Treatment	Stimulation	$[Ca^{2+}]_i$, nM		%Inc	*n*
		Baseline	Peak		
	Epo	38±2	135±11	271±24	23
	PBS	38±4	53±5	45±8*	10
U-73122					
10 μM	Epo	34±4	26±6	−17±11*	3
5 μM	Epo	44±4	58±7	31±11*	5
2.5 μM	Epo	33±1	38±3	13±12*	4
1 μM	Epo	35±4	75±19	99±32*	7
0.1 μM	Epo	41±3	123±13	198±17	5
U-73343					
10 μM	Epo	38±5	123±20	232±44	6
5 μM	Epo	41±2	133±14	226±44	4
2.5 μM	Epo	37±2	145±19	298±2	4
1 μM	Epo	37±3	172±10	370±30	5
0.1 μM	Epo	34±6	122±15	265±25	3

Fura red-loaded Chinese hamster ovary (CHO)-S cells transfected with transient receptor potential protein channel (TRPC)2 clone 14 (c14) and erythropoietin (Epo) receptor (Epo-R) were preincubated with 0–10 μM U-73122 or U-73343 for 25 min. Intracellular calcium concentration ($[Ca^{2+}]_i$) (mean ± SE, in nM) is shown at baseline, and the peak measurement was obtained after monitoring over 20 min after Epo stimulation (40 U/ml). % Increase above baseline (%Inc) represents peak $[Ca^{2+}]_i$ divided by baseline × 100%, − 100% (baseline). PLC, phospholipase C; *n*, number of cells studied. *$P \leq 0.001$, significant difference from Epo stimulated cells not treated with inhibitor.

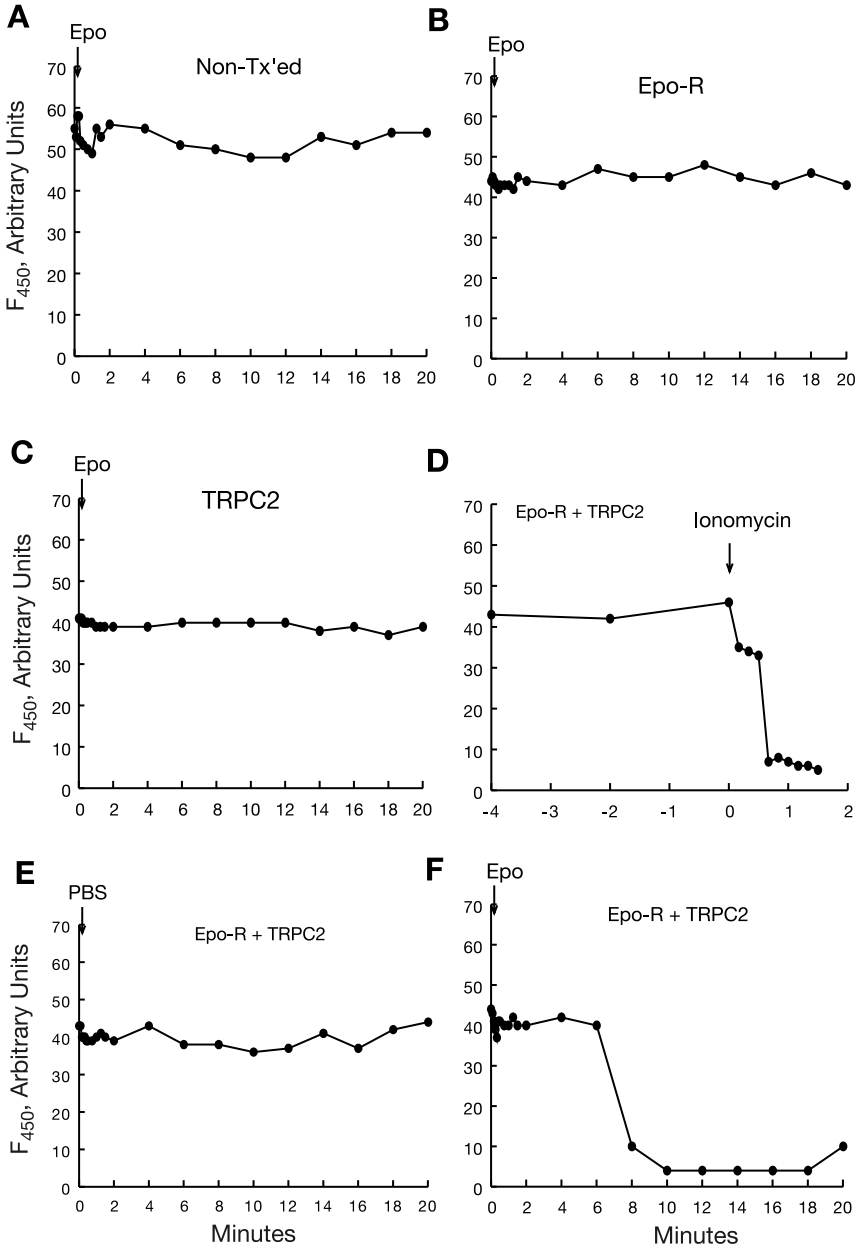

Fig. 3. Epo stimulation of Mn^{2+} flux through TRPC2. *A*: fluorescence intensity at 450 nm (F_{450}) near the Ca^{2+} isosbestic point was measured in fura red-loaded CHO-S cells with 0.68 mM $MnCl_2$ in the extracellular, nominally Ca^{2+}-free solution. Fluorescence was measured at baseline, at 5-s intervals for the first 30 s, at 15-s intervals for the next 75 s, and then at 2-min intervals until 20 min after stimulation with 40 U/ml of Epo. A representative time course of 8 nontransfected cells studied is shown. A representative time course is also shown for CHO-S cells transfected with Epo-R (*B*) (8 cells) or TRPC2 (*C*) (10 cells). *D*: CHO-S cells were transfected with Epo-R and TRPC2. After baseline measurements were obtained, cells were treated at 4 min with 1 μM ionomycin. A different time scale is shown here. *E*, *F*: fluorescence intensity was measured in CHO-S cells transfected with Epo-R and TRPC2, and treated with PBS (*E*) (14 cells) or 40 U/ml of Epo (*F*) (20 cells). A representative time course for 1 cell is shown with the same temporal sequence of measurements as described in *A*.

red fluorescence compared with nontransfected cells (Fig. 3*A*). The mean percentage decrease in fluorescence [mean fluorescence at maximal quench (F)/baseline fluorescence (F_0) × 100%] was 81 ± 3% for nontransfected cells (8 cells; Fig. 3*A*), 82 ± 4% for Epo-R (8 cells; Fig. 3*B*), and 85 ± 1% for TRPC2 transfected cells (10 cells; Fig. 3*C*). To confirm that Mn^{2+} influx was able to quench fura red fluorescence, CHO-S cells transfected with Epo-R and TRPC2 were treated with 1 μM ionomycin. This treatment resulted in a rapid decline in fura red fluorescence (mean $F/F_0 \times 100\% = 3 \pm 1\%$; 6 cells; Fig. 3*D*). To examine the ability of Epo to modulate Mn^{2+} influx, CHO-S cells transfected with Epo-R and TRPC2 were then stimulated with or without Epo in the presence of Mn^{2+}. Fura red fluorescence was measured at 5-s intervals for the first 30 s, at 15-s intervals for the next 75 s, and at 2-min intervals to 20 min. Cells stimulated with Epo demonstrated significant quenching of fura red fluorescence (mean $F/F_0 \times 100\% = 8 \pm 2\%$; $P < 0.0001$, 20 cells; Fig. 3*F*), compared with cells treated with PBS (mean $F/F_0 \times 100\% = 76 \pm 4\%$, 14 cells; Fig. 3*E*). Maximum quenching of fura red fluorescence occurred 10–16 min after treatment of Epo-R and TRPC2 transfected cells with Epo. These results demonstrate significant influx of Mn^{2+} in response to Epo.

To further characterize the rise in $[Ca^{2+}]_i$ modulated by Epo, CHO-S cells transfected with Epo-R and TRPC2 were stimulated by Epo in the presence of Ca^{2+}. Fura red fluorescence was monitored at time intervals similar to those described for the Mn^{2+} flux experiments. Figure 4*A* shows representative time courses of the response of one cell treated with PBS, and Fig. 4B shows representative time courses of one cell treated with Epo. Similar to previous observations (11, 12), the mean increase in $[Ca^{2+}]_i$ after Epo stimulation (32 ± 2 to 198 ± 24 nM, 15 cells studied) was significant ($P < 0.001$) compared with cells treated with PBS (36 ± 4 to 57 ± 7 nM; 9 cells

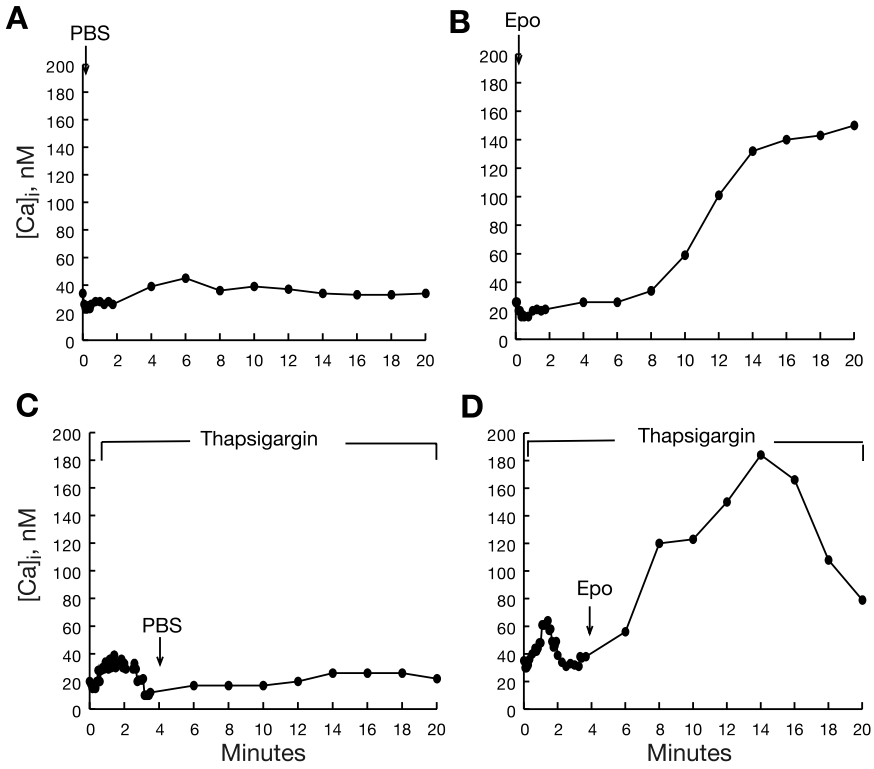

Fig. 4. Time course of $[Ca^{2+}]_i$ after Epo stimulation of CHO-S cells transfected with Epo-R and TRPC2. *A* and *B*: $[Ca^{2+}]_i$ was measured in representative CHO-S cells at baseline, at 5-s intervals for 30 s, at 15-s intervals for the next 90 s, and then at 2-min intervals until 20 min after stimulation with PBS (*A*) or Epo (40 U/ml) (*B*). *C* and *D*: $[Ca^{2+}]_i$ was measured in representative CHO-S cells treated with 3.5 μM thapsigargin at baseline, and at 4 min with PBS (*C*) or Epo (*D*). $[Ca^{2+}]_i$ was measured at baseline, at 5-s intervals for the first 4 min, and then at 2-min intervals to 20 min.

studied). The Epo-stimulated rise did not become significant until after 2 min of Epo stimulation and was sustained, reaching a plateau after 10 min.

This increase in $[Ca^{2+}]_i$ was previously shown to be dependent on external Ca^{2+} influx (11). To further examine the contribution of intracellular Ca^{2+} release to the rise in $[Ca^{2+}]_i$ stimulated by Epo, CHO-S cells transfected with Epo-R and TRPC2 were treated with thapsigargin to deplete intracellular Ca^{2+} stores. The ability of thapsigargin to release Ca^{2+}, resulting in an increase in $[Ca^{2+}]_i$ within 2 min, is shown in Fig. 4, *C* and *D*. Epo treatment at 4 min after $[Ca^{2+}]_i$ had returned to baseline resulted in a significant increase ($P < 0.01$) in $[Ca^{2+}]_i$ (27 ± 4 to 112 ± 11 nM; 9 cells) compared with cells treated with PBS (27 ± 5 to 51 ± 14 nM; 5 cells). Taken together, the Mn^{2+} flux and thapsigargin depletion data suggest that the major component of the Epo-stimulated rise in $[Ca^{2+}]_i$ through TRPC2 is extracellular Ca^{2+} influx.

PLC is required in Epo-modulated Ca^{2+} influx through TRPC2. To examine the mechanisms by which Epo modulates TRPC2, CHO-S cells transfected for 48 h with Epo-R and TRPC2 c14 were loaded with fura red in the presence of 0–10 μM of the active PLC inhibitor U-73122 or the inactive analog U-73343. Pretreatment with the active PLC inhibitor U-73122 inhibited the Epo-stimulated rise in $[Ca^{2+}]_i$ through TRPC2 at concentrations of 1 μM or greater (Table 1; $P < 0.01$), whereas the inactive analog U-73343 did not. These data strongly suggest that PLC is required for Epo-stimulated Ca^{2+} influx through TRPC2.

Depletion of PLCγ by RNAi suppresses Epo-stimulated Ca^{2+} influx. An alternative approach to using PLC inhibitors to examine the role of PLCγ in Epo-stimulated Ca^{2+} influx through TRPC2 is to use RNAi to downregulate PLCγ. For these experiments, we used HEK-293T cells and siRNA targeted to human PLCγ, the effectiveness of which was previously validated (24). HEK-293T cells were transfected with TRPC2 c14 and Epo-R as well as either siRNA directed to PLCγ or nonspecific control siRNA. The effectiveness of RNAi in altering expressed protein levels was monitored with Western blotting. Cotransfection of HEK-293T cells with siRNA directed to PLCγ resulted in significant suppression of endogenous PLCγ protein, compared with cells transfected with nonspecific control siRNA (Fig. 5). In contrast, expression of TRPC2 and Epo-R was equivalent in cells transfected with PLCγ siRNA and control siRNA, demonstrating the specificity of siRNA directed to PLCγ. The higher (165 kDa)

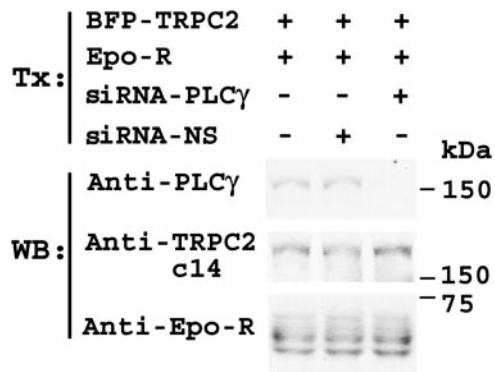

Fig. 5. Western blotting of human embryonic kidney (HEK)-293T cells transfected with RNA interference (RNAi). Lysates were prepared from HEK-293T cells transfected (Tx) with Epo-R and TRPC2 c14, with or without PLCγ1 *SMART*pool small interfering (siRNA) or nonspecific control *SMART*-pool siRNA. Blots were probed with anti-PLCγ1, anti-TRPC2 c14, or anti-Epo-R antibodies, followed by ECL.

molecular mass of TRPC2 c14 in Fig. 5 is the result of linkage to BFP.

To examine the functional consequences of suppression of PLCγ expression on Epo-induced $[Ca^{2+}]_i$ increase through TRPC2, HEK-293T cells transfected with TRPC2 and Epo-R, as well as either nonspecific or PLCγ-directed siRNA, were studied. Suppression of PLCγ resulted in significant inhibition of the Epo-stimulated $[Ca^{2+}]_i$ increase through TRPC2 (Table 2; $P < 0.0001$), whereas cotransfection with nonspecific siRNA did not. These data strongly support the conclusion that PLCγ is required for Epo-stimulated Ca^{2+} influx through TRPC2.

Coassociation of TRPC2, PLCγ, and Epo-R. Epo has been demonstrated to activate PLCγ1 and PLCγ2 (5, 26, 31, 40), and TRPC2 has several potential binding sites for PLCγ SH2 (centered at aa 530, 809) and SH3 (aa 259, 1,077) domains (Fig. 6) (41). Because PLC is involved in Epo-modulated Ca^{2+} influx through TRPC2, the ability of TRPC2 to interact with PLCγ directly was examined. Unfortunately, we were unable to immunoprecipitate TRPC2 c14 successfully with our anti-TRPC2 c14 antibody, possibly because anti-TRPC2 c14 is not a high-titer antibody or because the epitope recognized by this antibody is not accessible in the native protein. Therefore, CHO-S cells were transfected with V5-tagged TRPC2 c14 (pcDNA 3.1/V5-His TOPO), Epo-R (pcDNA3), PLCγ1 (pcDNA3), or all three plasmids. Immunoprecipitation studies were initially performed with preimmune rabbit serum or anti-V5 antibody using cell lysates of CHO-S cells expressing PLCγ1, V5-TRPC2 c14, and Epo-R. Western blotting performed on precipitates and supernatant fractions demonstrated that after immunoprecipitation with preimmune serum, PLCγ1, V5-TRPC2 c14, and Epo-R were not precipitated but remained in the supernatant fraction (Fig. 7). This demonstrates that little nonspecific binding occurred with our immunoprecipitation procedure. In contrast, anti-V5 immunoprecipitated V5-TRPC2 c14 as well as PLCγ1 and Epo-R, but not actin (Fig. 7). In these experiments, the quantity of protein present in the supernatant relative to that in the precipitate was difficult to compare because all of the precipitate but only 10% of the supernatant was loaded onto the gel.

To confirm the association of PLCγ1, V5-TRPC2 c14, and Epo-R, immunoprecipitation was performed with anti-V5, anti-PLCγ1, or anti-Epo-R antibodies (Fig. 8*A*). Western blotting demonstrated that anti-V5 antibody immunoprecipitated PLCγ1 and Epo-R in the presence of V5-TRPC2. Anti-PLCγ1 antibody immunoprecipitated V5-TRPC2 and Epo-R in the presence of PLCγ1, and anti-Epo-R antibody immunoprecipitated V5-TRPC2 and PLCγ1 in the presence of Epo-R (Fig. 8*A*). These results demonstrate that these three proteins coassociate. In these experiments, immunoprecipitation was also performed on CHO-S cells expressing PLCγ1, V5-TRPC2 c14, or Epo-R alone as controls for nonspecific binding. Epo-R and PLCγ1 were not immunoprecipitated by anti-V5 antibody in cells expressing Epo-R or PLCγ1 alone. Similarly, TRPC2 or Epo-R was not immunoprecipitated by anti-PLCγ1 antibody, nor was PLCγ1 or TRPC2 c14 immunoprecipitated by anti-Epo-R antibody, in lysates from transfections expressing each of these constructs alone (Fig. 8*A*).

As an additional control for specificity of immunoprecipitations, CHO-S cells were cotransfected with V5-tagged TRPV1 with a deletion of the PLCγ binding domain, PLCγ1, and Epo-R. Immunoprecipitation was performed with antibodies to V5, PLCγ1, and Epo-R. Western blotting demonstrated that

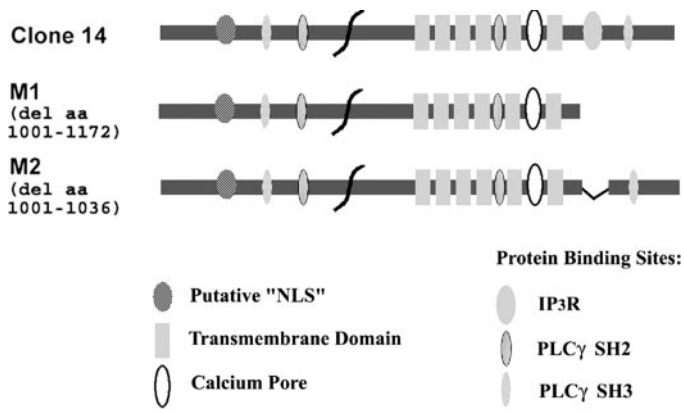

Fig. 6. Model of predicted functional domains on TRPC2 c14. Predicted functional domains on TRPC2 c14 and c14 with complete [mutant 1 (M1)] or partial [mutant 2 (M2)] deletions of IP_3R binding sites are shown.

Table 2. *Inhibition of Epo-stimulated calcium influx by RNAi directed to PLCγ*

		$[Ca^{2+}]_i$, nM			
RNAi	Stimulation	Baseline	Peak	%Inc	*n*
	Epo	43±2	173±18	322±46	17
	PBS	38±3	70±10	86±20*	9
NS	Epo	38±2	174±9	396±49	19
PLCγ1	Epo	39±2	67±5	74±10*	22

Human embryonic kidney (HEK)-293T cells were transfected with Epo-R and TRPC2 c14, with or without PLCγ1 *SMART*pool small interfering RNA (siRNA) or nonspecific control *SMART*pool siRNA (NS). At 48 h, cells were loaded with fura red. $[Ca^{2+}]_i$ (mean ± SE, in nM) was measured at baseline and by monitoring over 20 min after stimulation with 40 U/mL of Epo. %Increase above baseline (%Inc) = peak $[Ca^{2+}]_i$ divided by baseline × 100%, − 100% (baseline); *n*, number of cells studied. $*P \leq 0.001$, significant difference from cells transfected with wild-type TRPC2, not treated with RNA interference (RNAi) and stimulated with Epo.

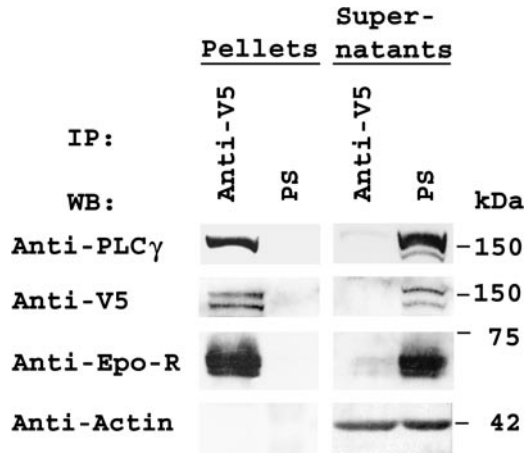

Fig. 7. Specificity of immunoprecipitation. PLCγ1, V5-TRPC2 c14, and Epo-R were expressed in CHO-S cells. Immunoprecipitation was performed with anti-V5 antibody or preimmune serum (PS). The entire immunoprecipitation pellet or 10% of the supernatant was loaded, and Western blotting was performed with anti-PLCγ1, anti-V5, anti-Epo-R, or anti-actin antibodies.

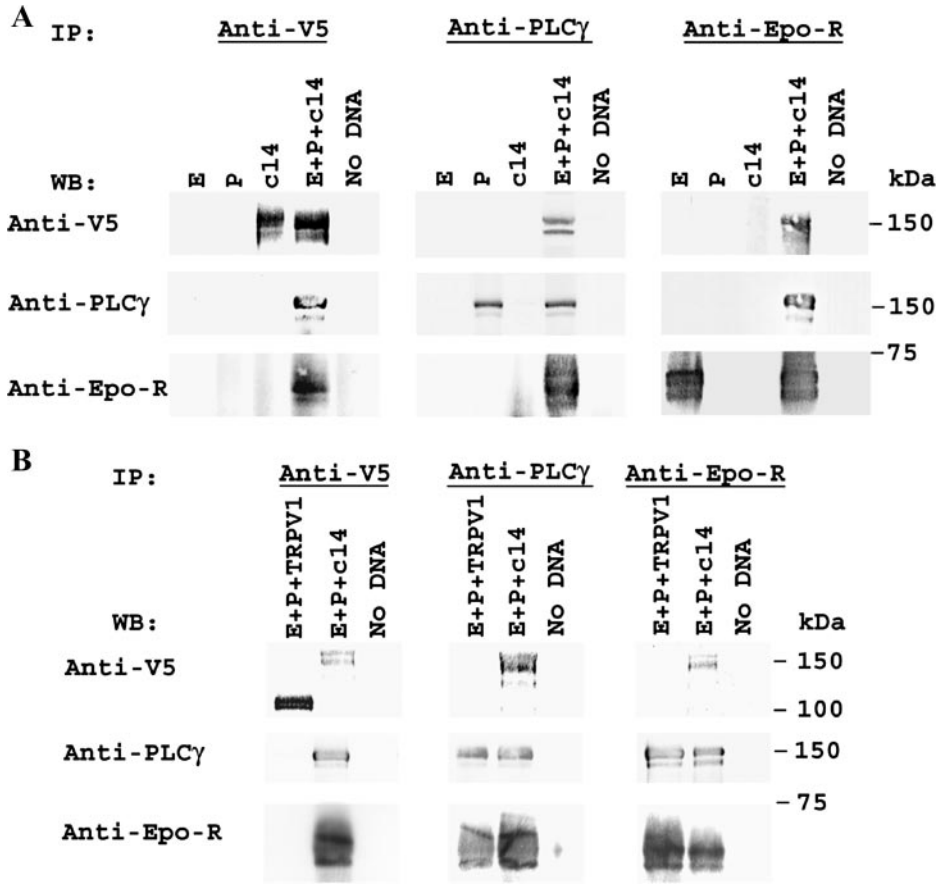

Fig. 8. Coimmunoprecipitation of TRPC2 c14, Epo-R, and PLCγ1. *A*: Epo-R (E), PLCγ1 (P), or V5-tagged TRPC2 c14 (c14) were expressed individually or together in CHO-S cells. Nontransfected CHO-S cells were used as a control (no DNA). Immunoprecipitation was performed on lysates from transfected or nontransfected cells with anti-V5, anti-PLCγ1, or anti-Epo-R antibodies. Western blotting of the precipitate was performed after each immunoprecipitation with anti-V5, anti-PLCγ1, or anti-Epo-R antibodies. *B*: CHO-S cells were transfected with Epo-R (E) and PLCγ1 (P), and TRPC2 c14 (c14) or mutant TRPV1 (V1) COOH-terminally tagged with V5. Nontransfected CHO-S cells were used as a control (no DNA). Immunoprecipitation was performed on lysates from transfected or nontransfected cells with anti-V5, anti-PLCγ1, or anti-Epo-R antibodies. Western blotting of the precipitate was performed after each immunoprecipitation with anti-V5, anti-PLCγ1, or anti-Epo-R antibodies.

anti-V5 antibody immunoprecipitated V5-TRPV1, but not PLCγ1 or Epo-R (Fig. 8*B*). Anti-PLCγ1 immunoprecipitated PLCγ1, Epo-R, and TRPC2 c14, but not V5-TRPV1, with a PLCγ SH3 binding site deletion. Anti-Epo-R immunoprecipitated Epo-R, TRPC2 c14, and PLCγ, but not V5-TRPV1. These results demonstrate the specific interaction between TRPC2 c14, PLCγ, and Epo-R.

IP3 receptors are involved in Epo activation of TRPC2. PLC activation results in production of IP_3. TRP channels were previously shown to interact with all IP_3R, and direct interaction with IP_3R may be a common mechanism for the activation of TRP channels (6, 42). TRPC2 has been reported to have two conserved IP_3R binding domains in its COOH terminus: one corresponding to aa 1001–1,036 of TRPC2 c14 and a second, less well defined site at aa 1,044–1,172 (42). To determine whether IP_3R binding sites are involved in Epo stimulation of TRPC2, two COOH-terminal mutants of TRPC2 were prepared (Fig. 6). Mutant 1 (M1) had a complete deletion of TRPC2 after aa 1,000 (aa 1,001–1,172), including both potential IP_3R binding sites. The second mutant (M2) had a deletion of the IP_3R binding site (aa 1,001–1,036) in the TRPC2 COOH terminus common to all TRPC proteins (42). Both mutants retained all six transmembrane domains and the putative Ca^{2+} pore (Fig. 6). CHO-S cells were cotransfected with Epo-R in pTracer-CMV and with BFP-tagged TRPC2 (in pQBI50) with or without deletion of the IP_3R binding sites. In cells transfected with Epo-R and TRPC2 c14 mutants with complete or partial deletion of the COOH-terminal IP_3R binding domains, no significant rise in $[Ca^{2+}]_i$ was observed in response to Epo stimulation, compared with control cells transfected with wild-type TRPC2 (Table 3). Expression of each of these channels in digital video imaging experiments was confirmed by BFP fluorescence. These data demonstrate a requirement for IP_3R binding domains in Epo-modulated Ca^{2+} influx through TRPC2.

Plasma membrane expression of each of these mutants was examined with confocal microscopy of cells transfected with TRPC2, IP_3R, and Epo-R. These studies demonstrated that wild type and mutant TRPC2 all localized partially at the plasma membrane and that the subcellular localizations of IP_3R type II and Epo-R were unchanged in CHO-S cells transfected with mutant TRPC2 (data not shown). These studies demon-

Table 3. *Epo activation of TRPC2 IP3R binding mutants*

TRPC2	Stimulation	$[Ca^{2+}]_i$, nM		%Inc	*n*
		Baseline	Peak		
wt	Epo	39±2	126±11	230±30	21
	PBS	35±4	48±5	38±6*	13
M1 del >aa 1,000	Epo	40±2	54±4	39±10*	15
M2 del aa 1,001–1,036	Epo	38±2	50±3	36±8*	18

CHO-S cells, transfected with Epo-R and TRPC2 with or without binding domain deletions, were loaded with fura red $[Ca^{2+}]_i$ (mean ± SE, nM), was measured at baseline and by monitoring over 20 min after stimulation with 40 U/ml Epo. %Increase above baseline (%Inc) = peak $[Ca^{2+}]_i$ divided by baseline × 100%, − 100% (baseline); *n*, number of cells studied. *$P \leq 0.0002$, significant difference from cells transfected with wild-type (wt) TRPC2 and stimulated with Epo.

strate that the absence of Ca^{2+} influx in digital video imaging experiments was not due to an inability of TRPC2 mutants to localize at the plasma membrane or mislocalization of IP_3R type II or Epo-R.

Coassociation of TRPC2 and IP3R. To determine whether TRPC2 interacts with IP_3R, immunoprecipitation experiments were performed. CHO-S cells were transfected with Epo-R (pcDNA3), IP_3R type II (pcDNA3), and/or V5-tagged TRPC2 c14 (pcDNA 3.1/V5-His TOPO). Immunoprecipitation was performed with antibodies to V5 or IP_3R type II using cell lysates of CHO-S cells expressing IP_3R, V5-TRPC2 c14, and Epo-R or CHO-S cells transfected with single plasmids as controls for specificity. Western blotting demonstrated that in cells transfected with wild-type V5-TRPC2, IP_3R type II, and Epo-R, anti-V5 antibody coimmunoprecipitated IP_3R and Epo-R (Fig. 9). Anti-IP_3R also immunoprecipitated TRPC2 and Epo-R in cotransfected cells. In contrast, IP_3R was not immunoprecipitated by anti-V5 antibody in cells expressing IP_3R alone, nor was V5-TRPC2 immunoprecipitated by anti-IP_3R antibody in cells expressing V5-TRPC2 alone.

To determine whether IP_3R binding to TRPC2 is abolished with mutants M1 and M2, CHO-S cells were transfected with V5-tagged TRPC2 c14 with mutations of the IP_3R binding site (pcDNA 3.1/V5-His TOPO), rat IP_3R type II (pcDNA3), and/or Epo-R (pcDNA3). Immunoprecipitation was performed with anti-V5 or anti-IP_3R type II antibodies. Anti-V5 immunoprecipitated V5-TRPC2 M1 (115 kDa; Fig. 10*A*) and anti-TRPC2 M2 (130 kDa; Fig. 10*B*). Similarly, anti-IP_3R antibody immunoprecipitated IP_3R. However, unlike the situation with wild-type TRPC2, TRPC2 M1 and M2 did not coimmunoprecipitate with IP_3R. These studies demonstrate that although mutant TRPC2 and IP_3R both localize partially to the plasma membrane, the direct association of IP_3R with TRPC2 is abolished in these two deletion mutants.

Endogenous association of IP3R, PLCγ, TRPC2, and Epo-R. To confirm the physiological significance of these findings, the ability of TRPC2 to interact with these proteins was examined in primary erythroid cells. Because anti-TRPC2 c14 antibody was unable to precipitate its target effectively, immunoprecipitation was performed with anti-Epo-R or anti-PLCγ1 antibodies using lysates of TER-119$^-$ erythroblasts. Immunoprecipitation was also performed with preimmune serum as a control. Western blots probed with anti-IP_3R, anti-PLCγ, anti-TRPC2 c14, or anti-Epo-R antibodies confirmed that these proteins associated endogenously (Fig. 11). These results are consistent with colocalization studies in primary erythroblasts using confocal microscopy.

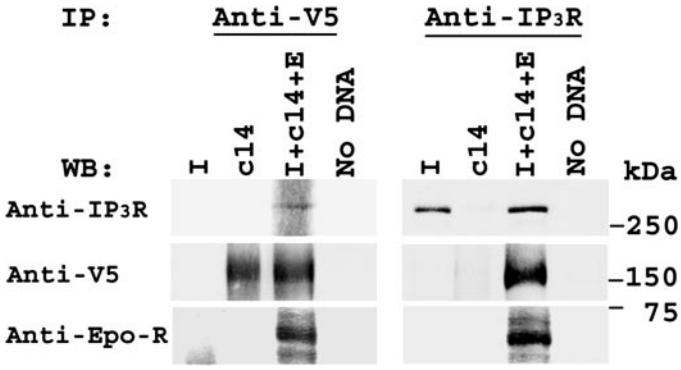

Fig. 9. Coimmunoprecipitation of TRPC2 c14, IP_3R, and Epo-R. IP_3R type II (I), V5-tagged TRPC2 (c14), and Epo-R (E) were expressed individually or together in CHO-S cells. Nontransfected CHO-S cells were used as controls (no DNA). Immunoprecipitation was performed on lysates from transfected or nontransfected cells with anti-V5 or anti-IP_3R type II antibodies. Western blotting of the immunoprecipitates was performed after each immunoprecipitation with anti-IP_3R type II, anti-V5, or anti-Epo-R antibodies, and detection was performed using ECL.

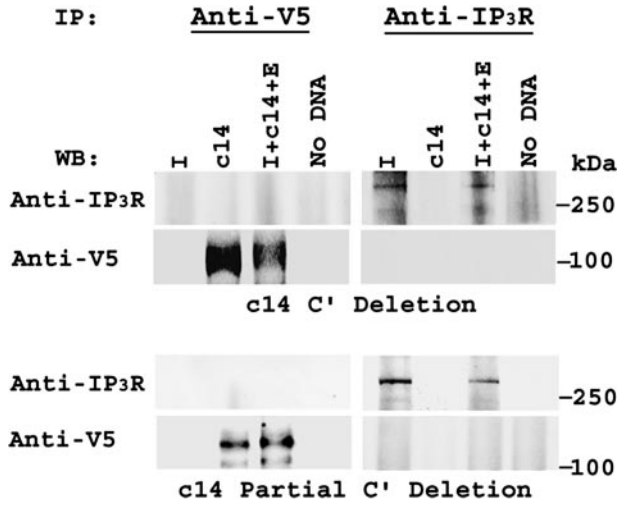

Fig. 10. Immunoprecipitation of TRPC2 c14 IP_3R binding mutants and IP_3R. IP_3R type II (I), V5-tagged TRPC2 M1 (*A*) and M2 (*B*) (c14), and Epo-R (E) were expressed individually or together in CHO-S cells. Immunoprecipitation was performed on lysates from transfected or nontransfected cells with anti-V5 or anti-IP_3R type II antibodies. Western blotting of the precipitated protein was performed after each immunoprecipitation with anti-IP_3R type II or anti-V5 antibodies.

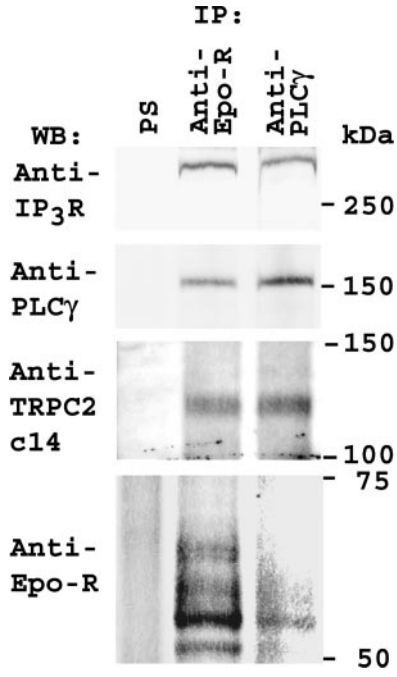

Fig. 11. Immunoprecipitation of Epo-R and PLCγ in TER-119$^-$ erythroblasts. Immunoprecipitation was performed on lysates from TER-119$^-$ erythroblasts with preimmune serum (PS), anti-Epo-R, or anti-PLCγ1 antibodies. Western blotting of eluates of bound protein was performed with anti-IP_3R, anti-PLCγ1, anti-TRPC2 c14, or anti-Epo-R antibodies.

DISCUSSION

Epo stimulates an increase in $[Ca^{2+}]_i$ in human and murine erythroid cells through voltage-independent ion channels (10, 14). Recently, a member of the Ca^{2+}-permeable transient receptor potential (TRP) channel family, TRPC2, was identified in primary erythroid cells, and Epo was shown to modulate Ca^{2+} influx through this channel (11, 12). The mechanisms through which Epo regulates Ca^{2+} influx through TRPC2 were explored in the present study. Our data strongly suggest that Epo modulation of TRPC2 requires PLCγ activation and direct interaction of TRPC2 with IP_3R. They also demonstrate that Epo-R, TRPC2, PLCγ1, and IP_3R associate to form a signaling complex.

A common characteristic of many TRPC channels is that they are activated through pathways involving PLC (36). Because Epo also activates PLCγ1 and PLCγ2 (5, 26, 31, 40), Epo activation of TRPC2 through a PLC-dependent pathway was explored. We have demonstrated that PLC activation by Epo is required for stimulation of Ca^{2+} influx in primary erythroid cells and for TRPC2 activation in a CHO-S model. Our evidence includes *1*) abolition of the Epo-induced $[Ca^{2+}]_i$ increase by either a specific PLC inhibitor (U-73122) or specific downregulation of PLCγ with RNAi and *2*) PLCγ association with Epo-R and TRPC2. Immunoprecipitation confirmed direct binding of PLCγ to TRPC2, which was predicted on the basis of a domain search (the Massachusetts Institute of Technology online Scansite Menu, available at: http://scansite.mit.edu/) indicating two potential PLCγ SH2 binding domains and two PLCγ SH3 binding domains on TRPC2. Our data are consistent with reports that demonstrated that PLCγ is involved in the activation of, and directly associates with, other TRPC. B cell receptor-induced activation of TRPC3 requires PLC (45), and PLCγ1 directly interacts with TRPC3 through the PLCγ1 SH3 domain (38). Further investigation is required to determine whether PLC modulates its effect on Epo-R regulated Ca^{2+} influx strictly by hydrolysis of PIP_2 to release IP_3 or whether it may also have a conformational or adapter role, as suggested in other studies in which catalytic phospholipase activity was not needed (38).

TRPC2 can be activated either by Ca^{2+} store release and/or by receptor-operated mechanisms (17, 44). Store depletion occurs after activation of PLC by appropriate receptor agonists, followed by production of IP_3, which then signals internal Ca^{2+} release from the endoplasmic reticulum through IP_3R. Depletion of Ca^{2+} from internal stores triggers a capacitative influx of extracellular Ca^{2+}. However, Ca^{2+} store release does not appear to play an important role in the activation of TRPC2 by Epo-R. In primary erythroid cells and in CHO-S cells transfected with TRPC2, a significant increase in $[Ca^{2+}]_i$ was not observed in the first 2 min after Epo addition, arguing against activation of TRPC2 by Ca^{2+} store release in these cells (Fig. 4) (12). Furthermore, when extracellular Ca^{2+} was substituted with Mn^{2+}, a slow quenching of fura red fluorescence, indicative of Mn^{2+} influx, was observed that was maximal after 10 min of Epo stimulation (Fig. 3). In addition, after thapsigargin depletion of intracellular Ca^{2+} stores, a significant rise in $[Ca^{2+}]_i$ was observed after treatment with Epo (Fig. 4). Consistent with these observations, in primary human erythroblasts in which Epo-responsive, voltage-independent Ca^{2+} channels have been demonstrated by single-channel recording (10), the increase in $[Ca^{2+}]_i$ after Epo stimulation required external Ca^{2+}, and no significant increase in $[Ca^{2+}]_i$ was observed in its absence (9). Similarly, the increase in $[Ca^{2+}]_i$ after Epo stimulation of CHO-S cells transfected with Epo-R and TRPC2 was dependent on extracellular Ca^{2+} (11). Although the lack of global increase in $[Ca^{2+}]_i$ in response to Epo in cells incubated in Ca^{2+}-free medium does not rule out a local release of Ca^{2+} that was effectively buffered, our experiments strongly suggest that the increase in $[Ca^{2+}]_i$ observed with Epo was mediated primarily through Ca^{2+} influx. These data are consistent with observations in the VNO (27), where TRPC2 regulates VNO sensory transduction independently of depletion of internal Ca^{2+} stores, which are absent in the sensory microvilli. The increase in $[Ca^{2+}]_i$ after Epo activation of TRPC2 was delayed, and this may be secondary to the interplay of several factors, including channel conductance, channel open probability, channel open time, and the rate at which Ca^{2+} is extruded from the cell or buffered in intracellular organelles.

TRPC interact with all IP_3R, and direct interaction of activated IP_3R with TRPC, altering TRPC conformation, has been proposed to be a common activation mechanism (4, 6, 13, 19, 20, 29, 42). In the present study, we have demonstrated that Epo-dependent activation of TRPC2 requires IP_3R binding to TRPC2. This is consistent with the report of Brann et al. (7), who demonstrated that IP_3R type III interacts with TRPC2 in the VNO. Previously, researchers at our laboratory (9) and others (32) were unable to demonstrate a global rise in IP_3 in primary human erythroid cells in response to Epo stimulation, although an increase in IP_3 in response to Epo stimulation was observed in UT-7 cells, a human Epo-dependent cell line (40). In the present study, we have demonstrate that IP_3R are in close proximity to PLCγ-coupled TRPC2. This would allow IP_3R exposure to a localized increase in IP_3 near the cell membrane that might escape detection in whole cell studies.

In this report, we demonstrate the colocalization of TRPC2, Epo-R, PLCγ1, and IP_3R type II at or near the plasma membrane of primary murine erythroid cells. We also demonstrate the coassociation of TRPC2 with Epo-R, PLCγ1 and IP_3R type II in erythroblasts and in transfected cells. In previous studies, Epo-R was shown to interact with PLCγ1 (31), and TRPC2 was shown to interact with IP_3R (7), in nonerythroid cells. An unexpected finding in the present study was the association of Epo-R with TRPC2 and IP_3R. Future studies are required to determine whether these associations represent direct interactions or whether adapter proteins such as PDZ domain-containing proteins serve to link the complex (25, 43, 46). The importance of the linkage of IP_3R to specific receptors, allowing IP_3 to be produced at required concentrations and precise locations, was demonstrated in neuronal cells for the B2 bradykinin receptor (13).

Our data demonstrate that Epo-R modulates TRPC2 activation through PLCγ and that interaction with IP_3R is required. They suggest that a signaling complex including Epo-R, TRPC2, PLCγ, and IP_3R is involved in the regulation of TRPC2. These data are consistent with a mechanism in which Epo stimulation of Epo-R results in activation of PLCγ and production of IP_3. Whether a conformational change in PLCγ has any direct influence on TRPC2 opening is unknown. In any case, IP_3 then interacts with IP_3R, which is in close proximity,

resulting in a conformational change in IP$_3$R and contributing to activation of TRPC2.

ACKNOWLEDGMENTS

We thank Dr. Lutz Birnbaumer for the gift of TRPC2 c14 cDNA as well as for helpful advice.

GRANTS

This work was supported by the National Institutes of Health Grants DK-46778 (to B. A. Miller) and HL-58672 (to J. Y. Cheung), by grants from the Geisinger Foundation and the Four Diamonds Fund of the Pennsylvania State University College of Medicine, and by the Canadian Institute for Health Research (to D. L. Barber). D. L. Barber is a National Cancer Institute of Canada Research Scientist.

REFERENCES

1. **Barber DL, Beattie BK, Mason JM, Nguyen MHH, Yoakim M, Neel BG, D'Andrea AD, and Frank DA.** A common epitope is shared by activated signal transducer and activator of transcription-5 (STAT5) and the phosphorylated erythropoietin receptor: implications for the docking model of STAT activation. *Blood* 97: 2230–2237, 2001.
2. **Beckman BS, Mallia C, and Clejan S.** Molecular species of phospholipids in a murine stem-cell line responsive to erythropoietin. *Biochem J* 314: 861–867, 1996.
3. **Berridge MJ, Lipp P, and Bootman MD.** The versatility and universality of calcium signalling. *Nat Rev Mol Cell Biol* 1: 11–21, 2000.
4. **Birnbaumer L, Boulay G, Brown D, Jiang M, Dietrich A, Mikoshiba K, Zhu X, and Qin N.** Mechanism of capacitative Ca^{2+} entry (CCE): interaction between IP3 receptor and TRP links the internal calcium storage compartment to plasma membrane CCE channels. *Recent Prog Horm Res* 55: 127–161, 2000.
5. **Boudot C, Petitfrère E, Kadri Z, Chretien S, Mayeux P, Haye B, and Billat C.** Erythropoietin induces glycosylphosphatidylinositol hydrolysis: possible involvement of phospholipase C-γ_2. *J Biol Chem* 274: 33966–33972, 1999.
6. **Boulay G, Brown DM, Qin N, Jiang M, Dietrich A, Zhu MX, Chen Z, Birnbaumer M, Mikoshiba K, and Birnbaumer L.** Modulation of Ca^{2+} entry by polypeptides of the inositol 1,4, 5-trisphosphate receptor (IP3R) that bind transient receptor potential (TRP): evidence for roles of TRP and IP3R in store depletion-activated Ca^{2+} entry. *Proc Natl Acad Sci USA* 96: 14955–14960, 1999.
7. **Brann JH, Dennis JC, Morrison EE, and Fadool DA.** Type-specific inositol 1,4,5-trisphosphate receptor localization in the vomeronasal organ and its interaction with a transient receptor potential channel, TRPC2. *J Neurochem* 83: 1452–1460, 2002.
8. **Caterina MJ, Schumacher MA, Tominaga M, Rosen TA, Levine JD, and Julius D.** The capsaicin receptor: a heat-activated ion channel in the pain pathway. *Nature* 389: 816–824, 1997.
9. **Cheung JY, Elensky MB, Brauneis U, Scaduto RC Jr, Bell LL, Tillotson DL, and Miller BA.** Ion channels in human erythroblasts: modulation by erythropoietin. *J Clin Invest* 90: 1850–1856, 1992.
10. **Cheung JY, Zhang XQ, Bokvist K, Tillotson DL, and Miller BA.** Modulation of calcium channels in human erythroblasts by erythropoietin. *Blood* 89: 92–100, 1997.
11. **Chu X, Cheung JY, Barber DL, Birnbaumer L, Rothblum LI, Conrad K, Abrasonis V, Chan YM, Stahl R, Carey DJ, and Miller BA.** Erythropoietin modulates calcium influx through TRPC2. *J Biol Chem* 277: 34375–34382, 2002.
12. **Chu X, Tong Q, Cheung JY, Wozney J, Conrad K, Mazack V, Zhang W, Stahl R, Barber DL, and Miller BA.** Interaction of TRPC2 and TRPC6 in erythropoietin modulation of calcium influx. *J Biol Chem* 279: 10514–10622, 2004.
13. **Delmas P, Wanaverbecq N, Abogadie FC, Mistry M, and Brown DA.** Signaling microdomains define the specificity of receptor-mediated InsP$_3$ pathways in neurons. *Neuron* 14: 209–220, 2002.
14. **Gillo B, Ma YS, and Marks AR.** Calcium influx in induced differentiation of murine erythroleukemia cells. *Blood* 81: 783–792, 1993.
15. **Harteneck C, Plant TD, and Schultz G.** From worm to man: three subfamilies of TRP channels. *Trends Neurosci* 23: 159–166, 2000.
16. **Hofmann T, Obukhov AG, Schaefer M, Harteneck C, Gudermann T, and Schultz G.** Direct activation of human TRPC6 and TRPC3 channels by diacylglycerol. *Nature* 397: 259–263, 1999.
17. **Jungnickel MK, Marrero H, Birnbaumer L, Lémos JR, and Floman HM.** Trp2 regulates entry of Ca^{2+} into mouse sperm triggered by egg ZP3. *Nat Cell Biol* 3: 499–502, 2001.
18. **Kina T, Ikuta K, Takayama E, Wada K, Majumdar AS, Weissman IL, and Katsura Y.** The monoclonal antibody TER-119 recognizes a molecule associated with glycophorin A and specifically marks the late stages of murine erythroid lineage. *Br J Haematol* 109: 280–287, 2000.
19. **Kiselyov K, Mignery GA, Zhu MX, and Muallem S.** The N-terminal domain of the IP$_3$ receptor gates store-operated hTrp3 channels. *Mol Cell* 4: 423–429, 1999.
20. **Kiselyov K, Xu X, Mozhayeva G, Kuo T, Pessah I, Mignery G, Zhu X, Birnbaumer L, and Muallem S.** Functional interaction between InsP$_3$ receptors and store-operated Htrp3 channels. *Nature* 396: 478–482, 1998.
21. **Klingmüller U.** The role of tyrosine phosphorylation in proliferation and maturation of erythroid progenitor cells: signals emanating from the erythropoietin receptor. *Eur J Biochem* 249: 637–647, 1997.
22. **Krystal G.** A simple microassay for erythropoietin based on ^{3}H-thymidine incorporation into spleen cells from phenylhydrazine treated mice. *Exp Hematol* 11: 649–660, 1983.
23. **Kurebayashi N, Harkins AB, and Baylor SM.** Use of fura red as an intracellular calcium indicator in frog skeletal muscle fibers. *Biophys J* 64: 1934–1960, 1993.
24. **Kwon YK, Jang HJ, Kole S, He HJ, and Bernier M.** Role of the pleckstrin homology domain of PLCγ1 in its interaction with the insulin receptor. *J Cell Biol* 163: 375–384, 2003.
25. **Li HS and Montell C.** TRP and the PDZ protein, INAD, form the core complex required for retention of the signalplex in *Drosophila* photoreceptor cells. *J Cell Biol* 150: 1411–1422, 2000.
26. **Liao HJ, Kume T, McKay C, Xu MJ, Ihle JN, and Carpenter G.** Absence of erythrogenesis and vasculogenesis in Plcg1-deficient mice. *J Biol Chem* 277: 9335–9341, 2002.
27. **Liman ER, Corey DP, and Dulac C.** TRP2: a candidate transduction channel for mammalian pheromone sensory signaling. *Proc Natl Acad Sci USA* 96: 5791–5796, 1999.
28. **Lintschinger B, Balzer-Geldsetzer M, Baskaran T, Graier WF, Romanin C, Zhu MX, and Groschner K.** Coassembly of Trp1 and Trp3 proteins generates diacylglycerol- and Ca^{2+}-sensitive cation channels. *J Biol Chem* 275: 27799–27805, 2000.
29. **Lockwich TP, Liu X, Singh BB, Jadlowiec J, Weiland S, and Ambudkar IS.** Assembly of Trp1 in a signaling complex associated with caveolin-scaffolding lipid raft domains. *J Biol Chem* 275: 11934–11942, 2000.
30. **Ma HT, Patterson RL, van Rossum DB, Birnbaumer L, Mikoshiba K, and Gill DL.** Requirement of the inositol trisphosphate receptor for activation of store-operated Ca^{2+} channels. *Science* 287: 1647–1651, 2000.
31. **Marrero MB, Venema RC, Ma H, Ling BN, and Eaton DC.** Erythropoietin receptor-operated Ca^{2+} channels: activation by phospholipase C-γ 1. *Kidney Int* 53: 1259–1268, 1998.
32. **Mason-Garcia M, Clejan S, Tou JS, and Beckman BS.** Signal transduction by the erythropoietin receptor: evidence for the activation of phospholipases A_2 and C. *Am J Physiol Cell Physiol* 262: C1197–C1203, 1992.
33. **Miller BA, Cheung JY, Tillotson DL, Hope SM, and Scaduto RC Jr.** Erythropoietin stimulates a rise in intracellular-free calcium concentration in single BFU-E derived erythroblasts at specific stages of differentiation. *Blood* 73: 1188–1194, 1989.
34. **Miller BA, Scaduto RC Jr, Tillotson DL, Botti JJ, and Cheung JY.** Erythropoietin stimulates a rise in intracellular free calcium concentration in single early human erythroid progenitors. *J Clin Invest* 82: 309–315, 1988.
35. **Minke B and Cook B.** TRP channel proteins and signal transduction. *Physiol Rev* 82: 429–472, 2002.
36. **Montell C.** Physiology, phylogeny, and functions of the TRP superfamily of cation channels. *Sci STKE* 2001: RE1, 2001.
37. **Montell C, Birnbaumer L, and Flockerzi V.** The TRP channels, a remarkably functional family. *Cell* 108: 595–598, 2002.
38. **Patterson RL, van Rossum DB, Ford DL, Hurt KJ, Bae SS, Suh PG, Kurosaki T, Snyder SH, and Gill DL.** Phospholipase C-γ is required for agonist-induced Ca^{2+} entry. *Cell* 111: 529–541, 2002.
39. **Ramos-Franco J, Bare D, Caenepeel S, Nani A, Fill M, and Mignery G.** Single-channel function of recombinant type 2 inositol 1,4, 5-trisphosphate receptor. *Biophys J* 79: 1388–1399, 2000.

40. **Ren HY, Komatsu N, Shimizu R, Okada K, and Miura Y.** Erythropoietin induces tyrosine phosphorylation and activation of phospholipase C-γ 1 in a human erythropoietin-dependent cell line. *J Biol Chem* 269: 19633–19638, 1994.
41. **Songyang Z, Shoelson SE, Chaudhuri M, Gish G, Pawson T, Haser WG, King F, Roberts T, Ratnofsky S, Lechleider RJ, Neel BJ, Birge RB, Fajardo JE, Chou MM, Hanafusa H, Schaffhausen B, and Cantley LC.** SH2 domains recognize specific phosphopeptide sequences. *Cell* 72: 767–778, 1993.
42. **Tang J, Lin Y, Zhang Z, Tikunova S, Birnbaumer L, and Zhu MX.** Identification of common binding sites for calmodulin and inositol 1,4,5-trisphosphate receptors on the carboxyl termini of trp channels. *J Biol Chem* 276: 21303–21310, 2001.
43. **Tang Y, Tang J, Chen Z, Trost C, Flockerzi V, Li M, Ramesh V, and Zhu MX.** Association of mammalian trp4 and phospholipase C isozymes with a PDZ domain-containing protein, NHERF. *J Biol Chem* 275: 37559–37564, 2000.
44. **Vannier B, Peyton M, Boulay G, Brown D, Qin N, Jiang M, Zhu X, and Birnbaumer L.** Mouse trp2, the homologue of the human trpc2 pseudogene, encodes mTrp2, a store depletion-activated capacitative Ca^{2+} entry channel. *Proc Natl Acad Sci USA* 96: 2060–2064, 1999.
45. **Venkatachalam K, Ma HT, Ford DL, and Gill DL.** Expression of functional receptor-coupled TRPC3 channels in DT40 triple receptor $InsP_3$ knockout cells. *J Biol Chem* 276: 33980–33985, 2001.
46. **Voltz JW, Weinman EJ, and Shenolikar S.** Expanding the role of NHERF, a PDZ-domain containing protein adapter, to growth regulation. *Oncogene* 20: 6309–6314, 2001.
47. **Witthuhn BA, Quelle FW, Silvennoinen O, Yi T, Tang B, Miura O, and Ihle JN.** JAK2 associates with the erythropoietin receptor and is tyrosine phosphorylated and activated following stimulation with erythropoietin. *Cell* 74: 227–236, 1993.
48. **Wu Y and Clusin WT.** Calcium transient alternans in blood-perfused ischemic hearts: observations with fluorescent indicator Fura Red. *Am J Physiol Heart Circ Physiol* 273: H2161–H2169, 1997.